Supplementary Information for

# A new strategy for hyperconjugative antiaromatic compounds utilizing negative charges: a dibenzo[*b*,*f*]silepinyl dianion

Shotaro Ito,[a] Youichi Ishii,[a] Kazuya Ishimura,[b] and Takuya Kuwabara*[,c]

[a]Department of Applied Chemistry, Faculty of Science and Engineering, Chuo University, 1-13-27, Kasuga, Bunkyo-ku, Tokyo 112-8551, Japan

[b]X-Ability, Co., Ltd., Ishiwata Building 3rd Floor, 4-1-5 Hongo, Bunkyo-ku, Tokyo 113-0033, Japan

[c]Department of Chemistry and Biochemistry, Graduate school of Humanities and Sciences, Ochanomizu University, 2-1-1, Otsuka, Bunkyo-ku, Tokyo 112-8610, Japan

Table of contents

**1. General considerations**

All manipulations were carried out under an argon atmosphere by using standard Schlenk techniques or a glovebox unless otherwise stated. $Et_2O$, THF, DME, $C_6D_6$ and THF-$d_8$ were distilled over potassium mirror. $Ph_2SiCl_2$ was purchased from Tokyo Chemical Industry (TCI). 2,2′-Dibromostilbene was synthesized according to the literature.[1] $^1H$ (500 MHz), $^{13}C\{^1H\}$(126 MHz), $^7Li\{^1H\}$ (194 MHz), and $^{29}Si\{^1H\}$ (99 MHz) NMR spectra were recorded on a JEOL ECZ-500 spectrometer at 20°C unless otherwise stated. Chemical shifts are reported in δ and referenced to residual $^1H$ and $^{13}C$ signals of deuterated solvents as internal standards or to the $^7Li\{^1H\}$ and the $^{29}Si$ NMR signal of LiCl in $D_2O$ ($\delta$ = 0.00) and $SiMe_4$ in $CDCl_3$ ($\delta$ = 0.00), respectively, as external standards. Elemental analyses were performed on a Perkin Elmer 2400 series II CHN analyzer. UV-vis absorption spectra were recorded on a SHIMADZU UV-1800 spectrophotometer.

**X-ray diffraction analysis**

Diffraction data for **1, 2** and **3** were collected on a VariMax Saturn CCD diffractometer with graphite-monochromated Mo Kα radiation (λ = 0.71075 Å) at –180 °C. Intensity data were corrected for Lorenz-polarization effects and for empirical absorption (REQAB).[2] All calculations were performed using the CrystalStructure[3] crystallographic software package except for refinements, which were performed using SHELXL-2018/3.[4] The positions of the non-hydrogen atoms were determined by SHELXT.[5] All non-hydrogen atoms were refined on $F_o^2$ anisotropically by full-matrix least-square techniques. All hydrogen atoms were placed at the calculated positions with fixed isotropic parameters.

**Theoretical studies**

Theoretical calculations were performed by using the *Gaussian* 16 Rev.C[6] for geometries and NICS values, and the Gaussian 09 Rev. E.01[7] for the anisotropy of the current (induced) density (ACID) analysis. The NICS and ACID data as well as molecular orbitals for **1**, **2**, **2'**, and **4** were calculated using optimized structures. The optimized structures of **1** and **2** are in good agreements with their X-ray structures. All local minima were confirmed by the vibrational frequency calculations with zero imaginary frequency, which was performed at the same levels for the optimization.

NICS and ACID calculations for **1**, and optimization for **2** were performed at the B3LYP[8] level of theory using 6-31G(d) basis sets.[8] The NICS values, NBO calculations, and ACID data for **2'** and **4** were calculated at the B3LYP level of theory using 6-31+G(d) basis sets. The external magnetic field of ACID calculations was applied in the direction almost orthogonal to three-ring planes, and current density vectors were plotted onto the isosurface of 0.03.

## 2. Synthesis and analytical data for the new compounds

**Synthesis of Diphenyldibenzosilepin 1.**

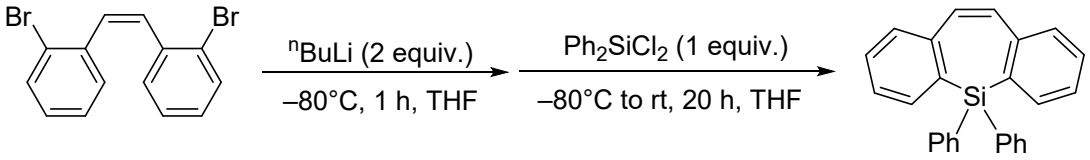


**1** (84% yield)

$^{n}$BuLi (1.59 M in hexanes, 3.70 mL, 5.88 mmol) was added to a THF solution (100 mL) of dibromostilbene (0.998 g, 2.95 mmol) in THF at −80 °C. After 1 hour, $Ph_2SiCl_2$ (0.60 mL, 0.722 g, 2.85 mmol) was added dropwise, then the mixture was allowed to gradually warm to room temperature and stirred for 20 hours. The solvent was removed in vacuo, and materials insoluble in $CH_2Cl_2$ were filtered off. The filtrate was concentrated and purified by recrystallization from $Et_2O$ to yield **1** as colorless crystals (0.890 g, 2.47 mmol, 84% yield). m.p. 203 °C; $^{1}$H NMR (500 MHz, $CDCl_3$): $\delta$ = 7.45–7.40 (m, 8H, Ar), 7.38–7.33 (m, 8H, Ar), 7.30–7.27 (m, 2H, Ar), 6.79 (s, 2H, vinyl); $^{13}$C{$^{1}$H} NMR (126 MHz, $CDCl_3$): $\delta$ = 142.5 (4°, $C_\alpha$ or $C_\beta$), 136.5 (3°), 136.0 (3°), 134.1 (4°, $C_\alpha$ or $C_\beta$), 133.1 (3°, *vinyl*), 132.8 (4°, $C_{ipso}$ *of Ph*), 130.2 (3°), 129.8 (3°), 129.7 (3°), 127.9 (3°), 127.2 (3°); $^{29}$Si{$^{1}$H} NMR (99 MHz, $CDCl_3$): $\delta$ = −13.9; Elemental analysis calcd (%) for $C_{26}H_{20}Si$ (**1**): C 86.62, H 5.59; found: C 86.24, H 5.55.

**Synthesis of lithium salt of 5,5-diphenyldibenzo[*b,f*]silepinyl dianion 2.**

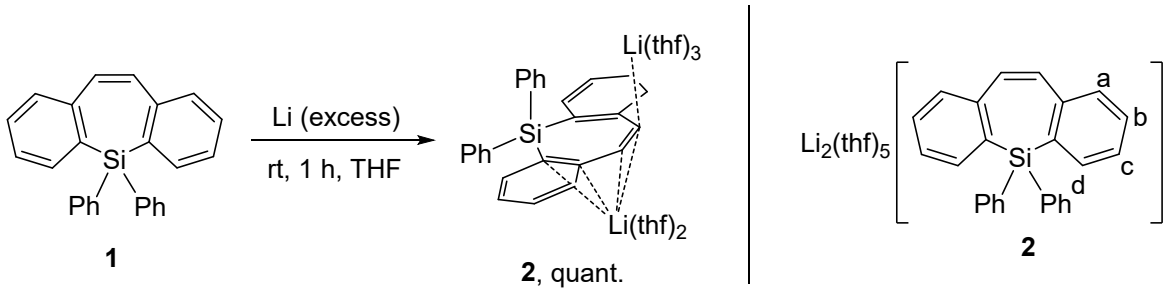


Lithium (16.6 mg, 2.39 mmol) was added to a solution of **1** (71.2 mg, 0.197 mmol) in THF (2 mL) at room temperature. After 1 hour, lithium was removed and the solvent was removed in vacuo to yield analytically pure **2** as black-purple powder (145.1 mg, 0.197 mmol, quant.) without any purifications. m.p. > 108 °C (decomp.); $^{1}$H NMR (500 MHz, THF-$d_8$): $\delta$ = 7.63–7.60 (m, 4H, *Ph*), 7.14–7.10 (m, 6H, *Ph*), 5.63 (dd, $^{3}J_{H-H}$ = 7 Hz, $^{4}J_{H-H}$ = 2 Hz, 2H, *fused benzene-d*), 5.34 (td, $^{3}J_{H-H}$ = 7 Hz, $^{4}J_{H-H}$ = 2 Hz, 2H, *fused benzene-b*), 4.99 (d, $^{3}J_{H-H}$ = 8 Hz, 2H, *fused benzene-a*), 4.22 (t, $^{3}J_{H-H}$ = 7 Hz, 2H, *fused benzene-c*) , 2.88 (s, 2H, *vinyl*); $^{13}$C{$^{1}$H} NMR (126 MHz, THF-$d_8$): $\delta$ = 147.9 ($C_\beta$), 143.4 (*ipso-Ph*), 142.6 (*fused benzene-d*), 137.4 (3°, *Ph*), 127.9 (*fused benzene-b*), 126.5 (3°, *para-Ph*), 126.3 (3°, *Ph*), 120.4 (*fused benzene-a*), 103.8 ($C_\alpha$), 97.4 (*fused benzene-c*), 78.4 (*vinyl*); $^{7}$Li{$^{1}$H} NMR (194 MHz, THF-$d_8$): $\delta$ = 0.21; $^{29}$Si{$^{1}$H} NMR (99 MHz, THF-$d_8$): $\delta$ = −31.0. Elemental analysis calcd (%) for $C_{46}H_{60}SiLi_2O_5$ (**2**): C 75.18, H 8.23; found: C 74.91, H 8.32.

**Reactivity of 2.**

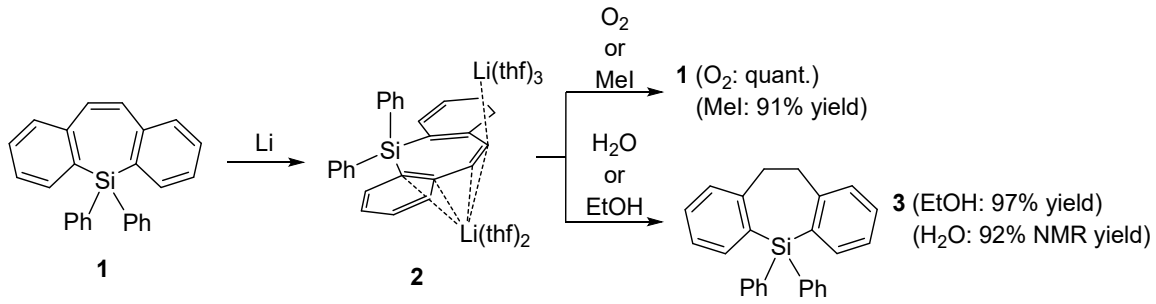


**$O_2$ quench:** Compound **2** was generated by the above method from **1** (30.0 mg, 0.0830 mmol) in THF (2 mL). After removal of excess lithium, $O_2$ gas was introduced to the Schlenk flask. The solvent was removed in vacuo to obtain white solids. Materials insoluble in $CH_2Cl_2$ were filtered off and the solvent was removed in vacuo to yield **1** as white powder (30.4 mg, 0.0841 mmol, quant.).

**MeI quench:** Compound **2** was generated by the above method from **1** (30.0 mg, 0.0830 mmol) in THF (2 mL). After removal of excess lithium, $CH_3I$ (0.1 mL, 228 mg, 1.61 mmol) was added dropwise. After 0.5 h, the solvent was removed in vacuo, and materials insoluble in $CH_2Cl_2$ were filtered off. The solvent was removed in vacuo and crude product was purified by preparative TLC (Hexane:$CH_2Cl_2$ = 4:1) to yield **1** as a white powder (27.2 mg, 0.0753 mmol, 91% yield).

**EtOH quench:** Compound **2** was generated by the above method from **1** (30.4 mg, 0.0841 mmol). After removal of excess lithium, EtOH (0.1 mL, 78.9 mg, 1.71 mmol) was added dropwise. After 0.5 hour, the solvent was removed in vacuo, and materials insoluble in $CH_2Cl_2$ were filtered off. The solvent was removed in vacuo to yield **3** as white powder (29.5 mg, 0.0815 mmol, 97% yield). m.p. 159 °C; $^1$H NMR (500 MHz, $CDCl_3$): $\delta$ = 7.43–7.40 (m, 6H, *Ar*), 7.36–7.32 (m, 8H, *Ar*), 7.21 (d, $^3J_{H-H}$ = 7 Hz, 2H, *Ar*), 7.15 (t, $^3J_{H-H}$ = 7 Hz, 2H, *Ar*), 3.20 (s, 4H, *methylene*); $^{13}$C{$^1$H} NMR (126 MHz, $CDCl_3$): $\delta$ = 150.5 (4°, $C_\alpha$ or $C_\beta$), 137.5 (3°), 136.2 (3°), 135.6 (4°), 133.1 (4°), 130.0 (3°), 129.5 (3°), 129.2 (3°), 127.9 (3°), 125.2 (3°), 36.8 (*methylene*); $^{29}$Si{$^1$H} NMR (99 MHz, $CDCl_3$): $\delta$ = −12.7; Elemental analysis calcd (%) for $C_{26}H_{22}Si$ (**3**): C 86.14, H 6.12; found: C 85.90, H 5.83.

**$H_2O$ quench:** Compound **2** was generated by the above method from **1** (30.1 mg, 0.0833 mmol). After removal of excess lithium, $H_2O$ (0.1 mL, 100 mg, 5.55 mmol) was added dropwise. After 0.5 hour, $MgSO_4$ was added to the solution, then the solvent was removed in vacuo. $MgSO_4$ and materials insoluble in $CH_2Cl_2$ were filtered off. The solvent was removed in vacuo to yield mixture of **1** and **3** as white powder (29.9 mg, 92% NMR yield for **3**). Compounds **1** and **3** could not be separated by column chromatography or recrystallization due to their similar chemical properties.

**3. Comparison of Si–C and C–C bond lengths of 1, 2 and 3, and HOMA values**

| | **1** | **2** | **3** |
|---|---|---|---|
| Si–C1/ Si–C6 | 1.8682(19)/1.8680(18) | 1.8424(14)/1.8470(14) | 1.875(2)/1.880(3) |
| Si–C15/Si–C21 | 1.8709(19/1.8748(19) | 1.8976(14)/1.8999(14) | 1.870(3)/1.880(2) |
| C1–C2/C5–C6 | 1.416(2)/1.413(2) | 1.4724(19)/1.4490(19) | 1.408(3)/1.418(3) |
| C2–C3/C4–C5 | 1.476(3)/1.465(3) | 1.390(2)/1.419(2) | 1.503(3)/1.514(3) |
| C3–C4 | 1.341(3) | 1.465(2) | 1.519(4) |
| C1–C7/C6–C14 | 1.401(3)/1.402(3) | 1.415(2)/1.4039(19) | 1.405(3)/1.401(3) |
| C7–C8/C14–C13 | 1.389(3)/1.386(3) | 1.382(2)/1.387(2) | 1.388(3)/1.393(4) |
| C8–C9/C13–C12 | 1.391(3)/1.382(3) | 1.420(2)/1.403(2) | 1.382(4)/1.388(4) |
| C9–C10/C12–C11 | 1.379(3)/1.382(3) | 1.358(2)/1.370(2) | 1.384(4)/1.373(4) |
| C10–C2/C5–C11 | 1.403(3)/1.408(2) | 1.457(2)/1.447(2) | 1.394(3)/1.404(3) |
| HOMA values of Ring a/b | 0.99/0.98 | 0.80/0.90 | 0.99/0.98 |

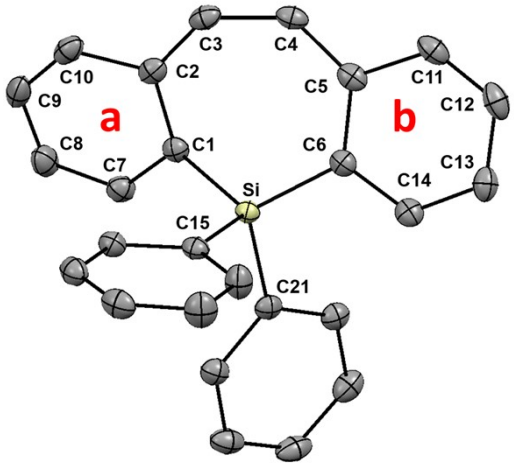


**Table S1** Comparison of Si–C and C–C bond lengths of **1**, **2** and **3**, and HOMA values for the six-membered rings.

**4. Comparison of $^1$H NMR chemical shifts of 2 and some dianionic aromatic/antiaromatic compounds**

Although $^1$H NMR signals of the dibenzosilepin core underwent upfield-shifts upon reduction, it is not clear whether these shifts are the diagnostic for the antiaromaticity of **2** because both anionic charges and paratropic ring current induce upfield shifts. However, it is worth comparing the $^1$H NMR data of **2** and other dianionic compounds having aromaticity or antiaromaticity (Table S2). The lithium salt of dibenzo[*a*,*e*]cyclooctatetraene dianion (**DBCOT$^{2-}$**),[9] and the lithium salt of phenanthrene dianions (**Phen$^{2-}$**, **Me$_2$Phen$^{2-}$**)[10] were selected as representatives for negatively charged aromatic and antiaromatic compounds, respectively. The former compound shows $^1$H NMR signals at common aromatic region [$\delta$ 6.98 (COT), 6.19 and 7.83 (fused benzene rings)] despite its negative charges. In contrast, $^1$H NMR signals of the latter compounds appeared in high-field region ranging from $\delta$ −1.14 to 2.75 for **Phen$^{2-}$** and $\delta$ 1.23 to 4.32 for **Me$_2$Phen$^{2-}$** due to the paratropic ring current as well as the negative charges. Considering that the $^1$H NMR signals for **2** recorded in THF-$d_8$ at room temperature ranged from $\delta$ 2.88 to 5.63, it is suggested that **2** has a weak antiaromatic character originating from its pseudo 16π-electron system involving negative hyperconjugation. The reason for the smaller upfield shifts in **2** compared to those in **Phen$^{2-}$** would originate from the hyperconjugation that is less effective than the conventional π-conjugation.

**Table S2** $^1$H NMR chemical shifts for dilithium salts of dianionic compounds having (anti)aromaticity recorded in THF-$d_8$.

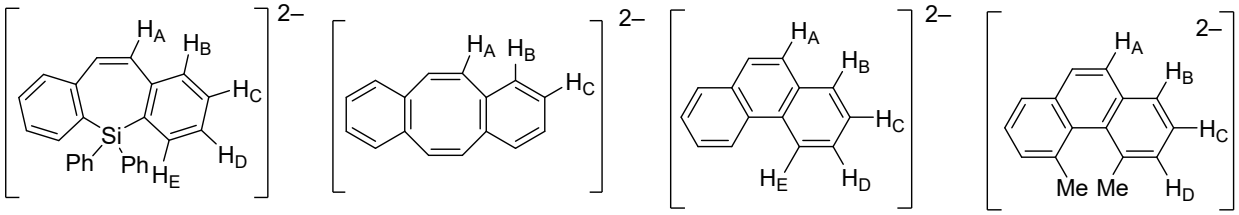


**2$^{2-}$** **DBCOT$^{2-}$** **Phen$^{2-}$** **Me$_2$Phen$^{2-}$**

| **2** | **DBCOT$^{2-}$** | **Phen$^{2-}$** | **Me$_2$Phen$^{2-}$** |
|---|---|---|---|
| 2.88 ($H_A$) | 6.98 ($H_A$) | −1.14 ($H_A$) | 1.23 ($H_A$) |
| 4.22 ($H_D$) | 6.19 ($H_B$ or $H_C$) | 0.62 ($H_B$) | 2.40 ($H_B$) |
| 4.99 ($H_B$) | 7.83 ($H_B$ or $H_C$) | 0.80 ($H_E$) | 3.62 ($H_D$) |
| 5.34 ($H_C$) | – | 1.69 ($H_D$) | 4.32 ($H_C$) |
| 5.63 ($H_E$) | – | 2.75 ($H_C$) | – |

**5. VT-$^1$H NMR measurements of 2 in THF-$d_8$**

VT-$^1$H NMR measurements in THF-$d_8$ were conducted. In the spectra recorded in THF-$d_8$, the signals of the fused benzene rings shifted to a low-field region by ca. 0.34–0.40 ppm upon heating from −80 °C to 60 °C (Figure S2). This temperature dependence suggests that antiaromaticity of **2** become weaker as the temperature increases. Our interpretation for this phenomenon at this point is as follows; the dibenzosilepinide core is more twisted at higher temperatures to minimize destabilization caused by its antiaromaticity. In fact, planarity of an antiaromatic molecule largely affect its $^1$H NMR chemical shifts. For instance, as mentioned in the previous page, the $^1$H NMR signals of **Me$_2$Phen$^{2-}$**, which has a highly twisted structure because of the steric repulsion between the Me groups, underwent notable downfield shifts compared to those of unsubstituted **Phen$^{2-}$** (Table S2).[9]

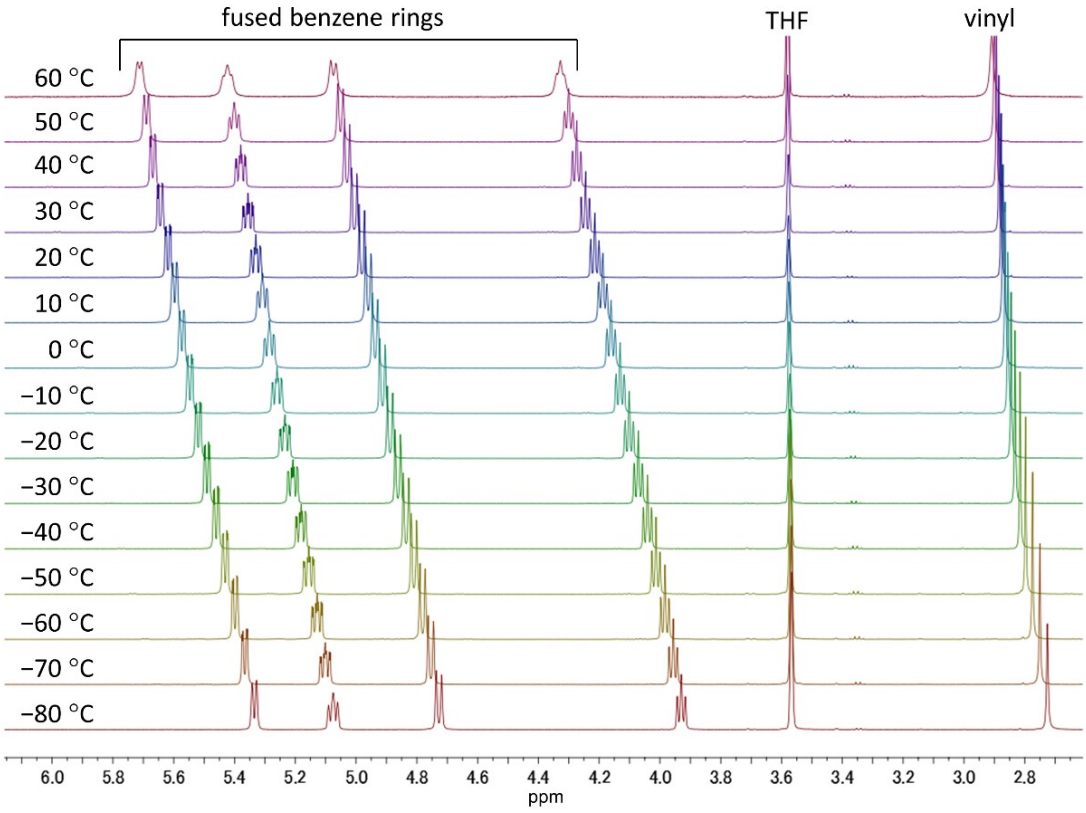


**Figure S1** VT-$^1$H NMR spectra of **2** in the temperature range of −80 to 60 °C in THF-$d_8$.

**6. Resonance structures, $^{13}$C NMR chemical shifts, and NPA charges of 2**

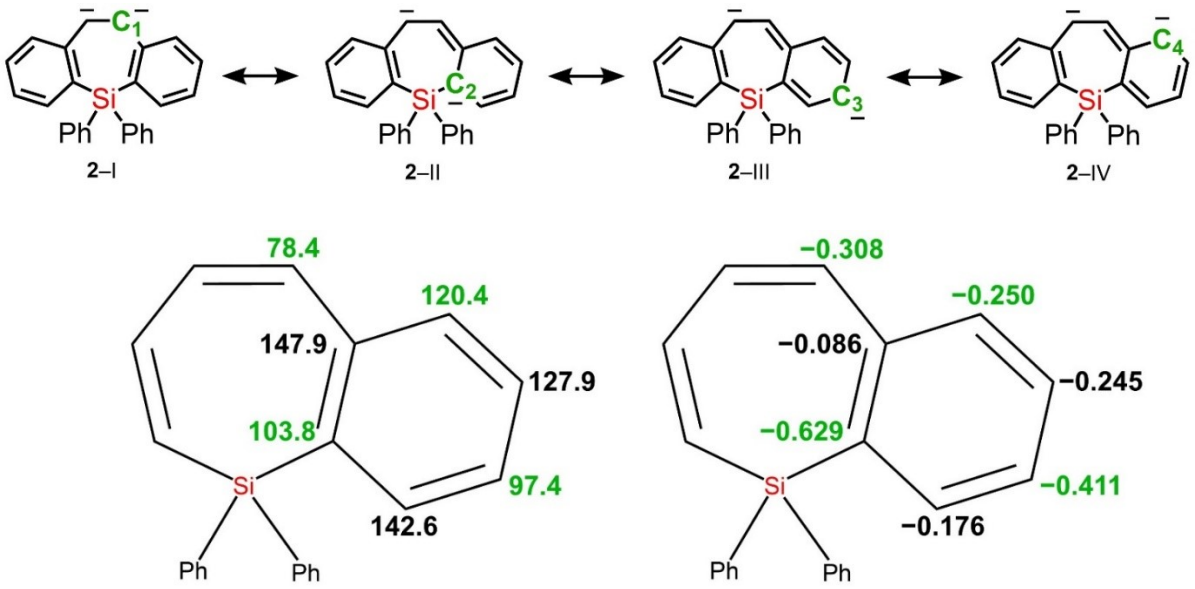


**Figure S2** Dominant resonance structures (top), $^{13}C\{^{1}H\}$ NMR chemical shifts of **2** in THF-$d_8$ (bottom, left) and the NPA charges of **2'** (bottom, right).

**7. VT-$^{7}$Li{$^{1}$H} NMR measurements of 2 in THF-$d_8$**

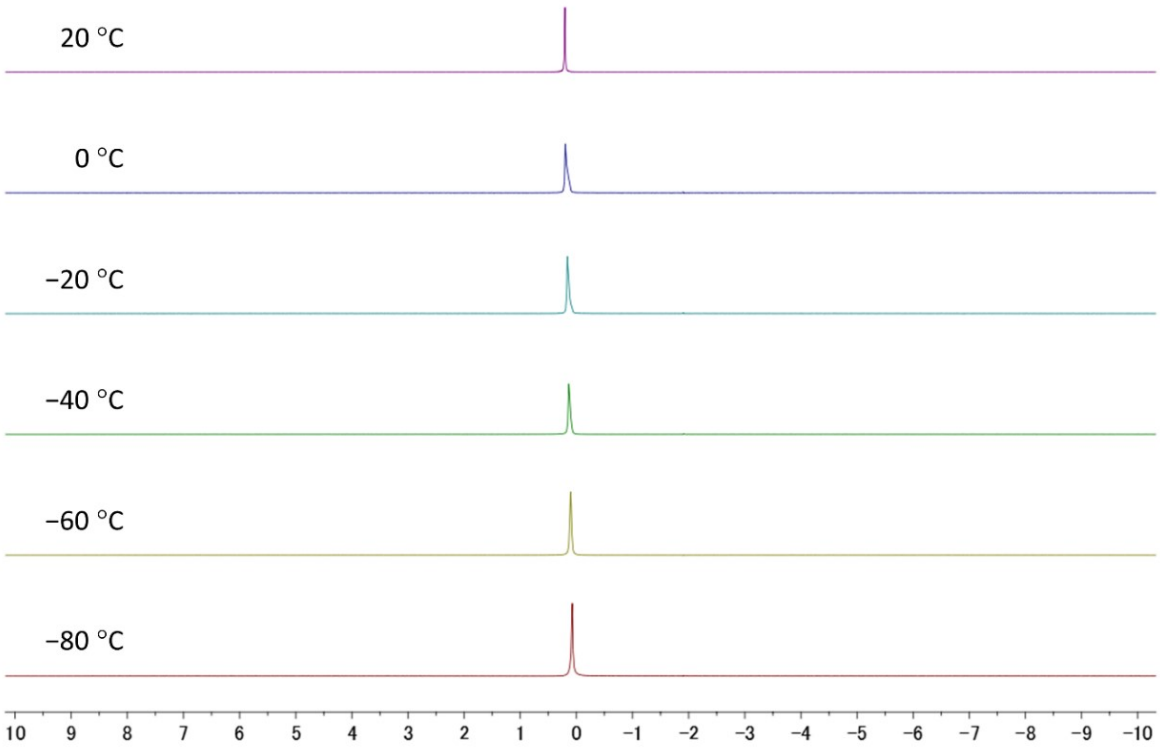


**Figure S3** VT-$^{7}$Li NMR spectra of **2** in THF-$d_8$.

**8. $NICS_{iso}$ values for 1, 2′, and a model compound 4**

$NICS_{iso}$ values[11] for **1**, **2′**, and dianion of dibenzothiepin **4**, which is a sulfur analog of **2′** as a model compound in which there is no contribution of hyperconjugation, were conducted (Table S3). Since these molecules are non-planar, NICS(+1) and NICS(−1) were defined as shown in Figure S4. As expected, the silepin and the flanking benzene rings of **1** are nonaromatic and aromatic, respectively. In stark contrast, the NICS values for both six- and seven-membered rings in **2′** were calculated to be positive, suggesting its antiaromatic character. It is noted that the NICS values of **4** much lower than **2′** are indicative of its nonaromatic nature. These results clearly indicate that the positive NICS values of **2′** originate from the negative hyperconjugation.

**Table S3** NICS(X) values for **1**, **2′** and **4**.

| | NICS(+1)<br>NICS(0)<br>NICS(−1)<br>six-membered rings | seven-membered ring |
|---|---|---|
| **1** | −10.6/−10.6 | −1.2 |
| | −7.7/−7.7 | 2.5 |
| | −10.7/−10.8 | −1.2 |
| **2′** | 7.0/8.0 | 2.1 |
| | 13.6/12.8 | 5.1 |
| | 8.2/7.5 | 4.2 |
| **4** | 1.5 | −4.6 |
| | 4.1 | −3.5 |
| | 2.0 | −3.6 |

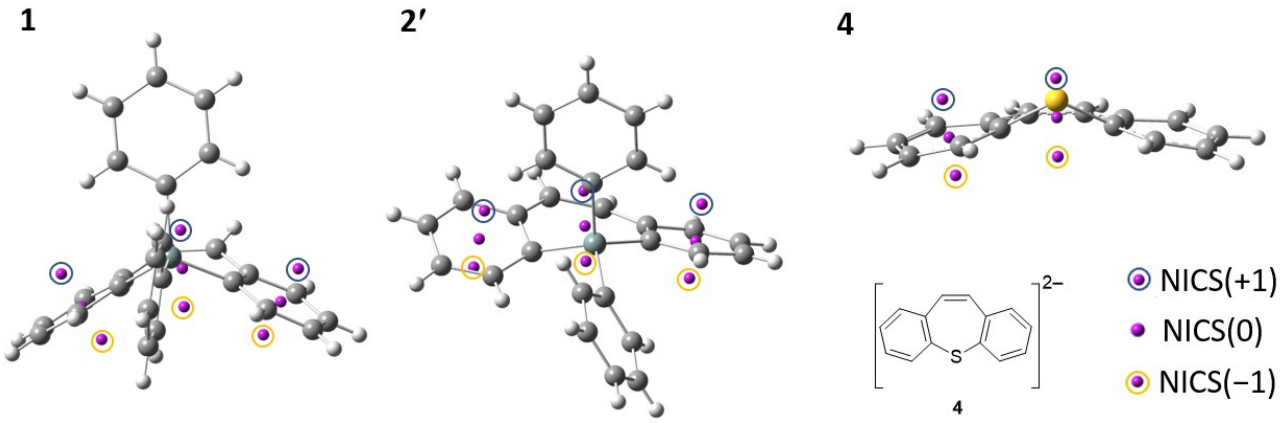


**Figure S4** The positions for the dummy atoms for the NICS calculations.

**9. Important molecular orbitals to understand the electronic structures of 1 and 2**

Figure S5 illustrates the frontier MOs for **1**, **2**, and **2′**. Since compound **2** is a two-electron reduced form of **1**, the HOMO and HOMO−1 of **2** essentially correspond to the LUMO and HOMO of **1**, respectively. In contrast to the orbital overlap between the π-clouds and the σ*(Si–Ph) orbital confirmed in the HOMO−1 of **2** and **2′**, no such overlap was observed in the HOMO of **1**, suggesting that the negative charges are essential to realize the hyperconjugation in this system.

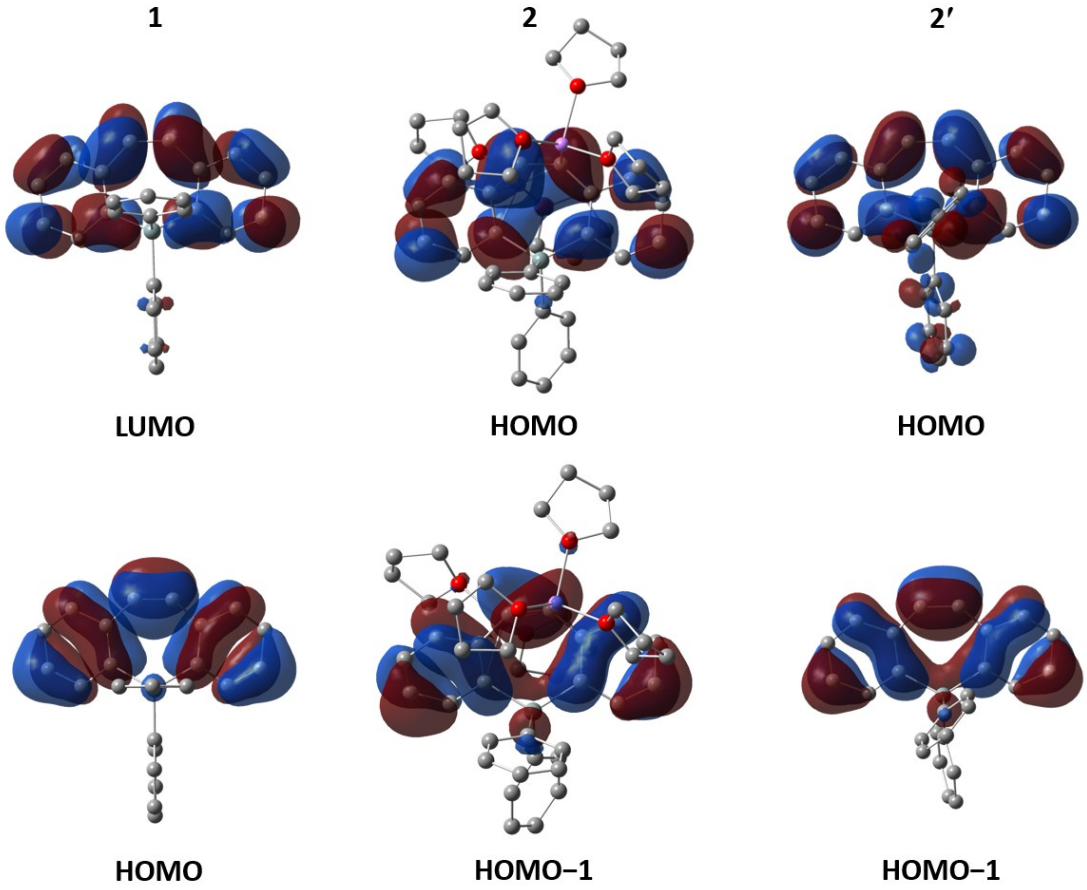


**Figure S5** Frontier MOs of **1**, **2**, and **2′** (isovalue = 0.02).

## 10. X-ray crystallographic data for 1, 2 and 3

**Table S4** X-ray crystallographic data for **1**, **2** and **3**.

| | **1** | **2** | **3** |
|---|---|---|---|
| CCDC | 2100087 | 2100088 | 2100091 |
| formula | $C_{26}H_{20}Si$ | $C_{46}H_{60}Li_2O_5Si$ | $C_{26}H_{22}Si$ |
| fw | 360.51 | 734.91 | 362.52 |
| crystal size | 0.08 × 0.07 × 0.06 | 0.15 × 0.09 × 0.07 | 0.09 × 0.05 × 0.05 |
| crystal system | triclinic | monoclinic | monoclinic |
| space group | *P*-1 | $P2_1/n$ | $P2_1/n$ |
| *a* [Å] | 9.1512(14) | 10.6771(12) | 8.9514(18) |
| *b* [Å] | 10.0552(16) | 23.008(2) | 19.204(4) |
| *c* [Å] | 11.032(2) | 16.8602(18) | 11.397(2) |
| *α* [deg] | 79.734(7) | 90 | 90 |
| *β* [deg] | 81.052(8) | 98.541(2) | 98.546(4) |
| *γ* [deg] | 74.730(8) | 90 | 90 |
| *V* [Å$^3$] | 957.3(3) | 4095.9(8) | 1937.4(7) |
| *Z* | 2 | 4 | 4 |
| $\rho_{calcd}$ [g cm$^{-3}$] | 1.251 | 1.192 | 1.243 |
| *F*(000) | 380 | 1584 | 768 |
| $\mu$ [cm$^{-1}$] | 1.3 | 1.02 | 1.29 |
| transmission factors range | 0.8544– 1 | 0.8544– 1 | 0.8544 – 1 |
| index range | -10 ≤ h ≤ 11<br>-12 ≤ k ≤ 12<br>-12 ≤ l ≤ 13 | -10 ≤ h ≤ 13<br>-29≤ k ≤ 29<br>-21 ≤ l ≤ 21 | -11 ≤ h ≤ 10<br>10 ≤ h ≤ -24<br>-24 ≤ h ≤ 24 |
| no. reflections | 7343 | 32961 | 15666 |
| unique ($R_{int}$) | 3858 (0.0322) | 9361 (0.0375) | 4365 (0.0748) |
| $I > 2\sigma(I)$ | 2719 | 7798 | 3034 |
| no. parameters | 244 | 520 | 245 |
| $R_1$ ($I > 2\sigma(I)$)[a] | 0.045 | 0.0494 | 0.0665 |
| $wR_2$ (all data)[b] | 0.1109 | 0.1285 | 0.1568 |
| GOF [c] | 1.009 | 1.053 | 1.048 |
| max diff peak / hole [e Å$^{-3}$] | 0.271/-0.359 | 0.285/-0.352 | 0.293/-0.358 |

[a] $R1 = \Sigma||F_o| - |F_c||/\Sigma|F_o|$. [b] $wR2 = [\Sigma\{w(F_o^2 - F_c^2)^2\}/\Sigma w(F_o^2)^2]^{1/2}$, $w = 1/[\sigma^2F_o^2 + (aP)^2 + bP]$ ($a$ and $b$ are constants suggested by the refinement program; $P = [\max(F_o^2,0) + 2F_c^2]/3$). [c] $GOF = [\Sigma w(F_o^2 - F_c^2)^2/(N_{obs} - N_{params})]^{1/2}$.

**11. Cartesian coordinates for 1, 2, 2′ and 4**

**Table S5** Cartesian coordinates for **1**.

$E_{total}$ = -1292.004537 Hartree

| | | | |
|---|---|---|---|
| Si | 0.195113 | -0.000118 | 0.00988 |
| C | -0.588265 | -1.530735 | 0.77928 |
| C | -0.586987 | 1.531084 | 0.779403 |
| C | 0.214808 | -2.586784 | 1.24507 |
| H | 1.295776 | -2.483581 | 1.212535 |
| C | -1.998066 | 1.686235 | 0.830124 |
| C | -1.999492 | -1.684611 | 0.829964 |
| C | 0.217051 | 2.586366 | 1.24529 |
| H | 1.297921 | 2.482181 | 1.212757 |
| C | -0.097618 | 0.000051 | -1.859661 |
| C | 2.999795 | -0.00068 | -0.690539 |
| H | 2.656981 | -0.000183 | -1.721793 |
| C | -0.329049 | 3.772099 | 1.736367 |
| H | 0.322393 | 4.57005 | 2.083034 |
| C | 2.058099 | -0.000867 | 0.353969 |
| C | -2.534874 | -2.901085 | 1.301788 |
| H | -3.615246 | -3.025285 | 1.322554 |
| C | -0.189887 | -1.204195 | -2.581262 |
| H | -0.136314 | -2.153894 | -2.05373 |
| C | -2.532353 | 2.903130 | 1.302093 |
| H | -3.612615 | 3.028281 | 1.322915 |
| C | -1.718631 | -3.929806 | 1.75825 |
| H | -2.162408 | -4.851303 | 2.126251 |
| C | 2.551012 | -0.001533 | 1.674839 |
| H | 1.855273 | -0.001705 | 2.511553 |
| C | -2.980406 | 0.678491 | 0.409111 |
| H | -3.932603 | 1.121927 | 0.11827 |
| C | 2.980961 | -0.675979 | 0.409037 |
| H | -3.933522 | -1.118592 | 0.118128 |
| C | -1.715175 | 3.931076 | 1.75863 |
| H | -2.158114 | 4.85294 | 2.126722 |
| C | 4.372646 | -0.001123 | -0.431366 |
| H | 5.079027 | -0.000969 | -1.257804 |
| C | -0.332362 | -3.772072 | 1.736034 |
| H | 0.318359 | -4.570634 | 2.082642 |
| C | -0.188485 | 1.204399 | -2.581263 |
| H | -0.133816 | 2.154043 | -2.053732 |
| C | -0.445426 | 0.000254 | -4.662477 |
| H | -0.581050 | 0.000328 | -5.741163 |
| C | -0.360834 | -1.207149 | -3.9666910 |
| H | -0.432112 | -2.150777 | -4.502072 |
| C | 3.920860 | -0.001984 | 1.939804 |
| H | 4.274306 | -0.002494 | 2.967956 |
| C | 4.836011 | -0.001777 | 0.884341 |

**Table S6-1** Cartesian coordinates for **2**.

$E_{total}$ = -2468.881510 Hartree

| | | | |
|---|---|---|---|
| Si | -1.336557 | -1.462434 | 0.185844 |
| C | -1.520342 | 0.044772 | 1.274385 |
| C | -0.348284 | 0.906590 | 1.518825 |
| C | 0.546476 | 1.301598 | 0.513889 |
| H | 1.270166 | 2.056864 | 0.841471 |
| C | 0.505825 | 1.141267 | -0.952710 |
| H | 1.015235 | 1.960481 | -1.468786 |
| C | 0.101747 | 0.098947 | -1.836837 |
| C | -0.587689 | -1.137192 | -1.496652 |
| C | -2.548895 | 0.041534 | 2.250194 |
| H | -3.429539 | -0.572112 | 2.062658 |
| C | -2.471890 | 0.724416 | 3.459333 |
| H | -3.282006 | 0.680359 | 4.181562 |
| C | -1.244006 | 1.366889 | 3.778002 |
| H | -1.108382 | 1.807401 | 4.765854 |
| C | -0.217646 | 1.433832 | 2.866649 |
| H | 0.706477 | 1.948022 | 3.133360 |
| C | 0.407233 | 0.270300 | -3.241075 |
| H | 0.866957 | 1.211005 | -3.547647 |
| C | 0.161038 | -0.695776 | -4.195185 |
| H | 0.427248 | -0.497506 | -5.233217 |
| C | -0.422260 | -1.928527 | -3.839366 |
| H | -0.625654 | -2.693782 | -4.582773 |
| C | -0.790316 | -2.101254 | -2.504163 |
| H | -1.301977 | -3.025747 | -2.237321 |
| C | -0.296466 | -2.737272 | 1.179981 |
| C | -0.213129 | -2.672736 | 2.584541 |
| H | -0.699207 | -1.853936 | 3.109177 |
| C | 0.484093 | -3.635846 | 3.321412 |
| H | 0.524441 | -3.561470 | 4.406211 |
| C | 1.123308 | -4.692232 | 2.670069 |
| C | 0.351306 | -3.817879 | 0.549759 |
| H | 0.301316 | -3.910343 | -0.532796 |
| C | -3.036157 | -2.326855 | -0.034280 |
| C | -5.583085 | -3.554610 | -0.290742 |
| H | -6.557372 | -4.027402 | -0.390209 |
| C | -5.076249 | -2.761479 | -1.321219 |
| H | -5.653101 | -2.620240 | -2.233055 |
| C | -3.822774 | -2.158000 | -1.189178 |
| H | -3.435202 | -1.564313 | -2.012477 |
| Li | -1.459906 | 1.989595 | -0.148115 |
| O | -1.800231 | 3.826967 | 0.630056 |
| C | -0.798360 | 4.631019 | 1.291111 |
| H | -0.521198 | 5.455636 | 0.619922 |
| H | 0.075918 | 4.000576 | 1.467924 |
| C | -1.448607 | 5.142381 | 2.578561 |
| H | -1.034000 | 6.101435 | 2.904945 |
| H | -1.310108 | 4.408164 | 3.378638 |
| C | -2.930855 | 5.220480 | 2.182542 |
| H | -3.131446 | 6.136579 | 1.613513 |
| H | -3.608612 | 5.195827 | 3.041181 |
| C | -3.081880 | 3.987376 | 1.291344 |
| H | -3.284925 | 3.086934 | 1.884034 |
| H | -3.844891 | 4.094071 | 0.515903 |
| O | -2.984126 | 2.092212 | -1.467503 |
| C | -4.294976 | 1.491481 | -1.326787 |
| H | -4.952339 | 2.192085 | -0.798064 |
| H | -4.177800 | 0.591536 | -0.718057 |
| C | -4.790936 | 1.186568 | -2.752587 |
| H | -5.290272 | 0.215123 | -2.807832 |
| H | -5.505144 | 1.949529 | -3.083608 |
| C | -3.506696 | 1.253003 | -3.598700 |
| H | -2.962880 | 0.303163 | -3.576285 |
| H | -3.697659 | 1.516220 | -4.643888 |
| C | -2.700591 | 2.318607 | -2.862726 |
| H | -1.621067 | 2.223325 | -2.995257 |
| H | -3.019275 | 3.334941 | -3.140095 |

**Table S6-2** Cartesian coordinates for **2**.

| | | |
|---|---|---|
| Li 2.596637 | 0.379102 | -0.250808 |
| O 3.556665 | 0.028708 | 1.534802 |
| C 3.975546 | 1.061177 | 2.452713 |
| H 3.240318 | 1.875319 | 2.419369 |
| H 4.945130 | 1.447053 | 2.119778 |
| C 4.021182 | 0.407256 | 3.837351 |
| H 3.827459 | 1.124832 | 4.640464 |
| H 5.004495 | -0.044633 | 4.015940 |
| C 2.941453 | -0.678860 | 3.714506 |
| H 3.063408 | -1.494372 | 4.433089 |
| H 1.942107 | -0.249738 | 3.843637 |
| C 3.125874 | -1.147013 | 2.273193 |
| H 3.910033 | -1.911881 | 2.191378 |
| H 2.208993 | -1.521116 | 1.816591 |
| O 3.762800 | 1.922744 | -1.032898 |
| C 3.966435 | 1.872855 | -2.469166 |
| H 3.258940 | 1.155157 | -2.889533 |
| H 4.988764 | 1.520740 | -2.658021 |
| C 3.765211 | 3.304024 | -2.970020 |
| H 4.336649 | 3.511019 | -3.879786 |
| H 2.705869 | 3.487830 | -3.183211 |
| C 4.219159 | 4.135931 | -1.761174 |
| H 3.817127 | 5.153473 | -1.757230 |
| H 5.313270 | 4.200853 | -1.728115 |
| C 3.695751 | 3.297576 | -0.593773 |
| H 4.291959 | 3.393877 | 0.318510 |
| H 2.651615 | 3.543891 | -0.361607 |
| O 3.492117 | -1.124760 | -1.236625 |
| C 2.862894 | -2.213111 | -1.975062 |
| H 2.208033 | -1.778525 | -2.730669 |
| H 2.255797 | -2.792090 | -1.273086 |
| C 4.019869 | -3.039722 | -2.534839 |
| H 4.363434 | -2.628572 | -3.492067 |
| H 3.740242 | -4.084946 | -2.696795 |
| C 5.097589 | -2.856872 | -1.455517 |
| H 1.664539 | -5.443123 | 3.241219 |
| C 1.053311 | -4.781611 | 1.277665 |
| H 1.540107 | -5.605551 | 0.759829 |
| C -3.568117 | -3.141985 | 0.983603 |
| H -2.988104 | -3.318266 | 1.886276 |
| C -4.822550 | -3.744330 | 0.864150 |
| H -5.202302 | -4.368336 | 1.670082 |
| H 6.113024 | -3.060480 | -1.809723 |
| H 4.895833 | -3.513684 | -0.600994 |
| C 4.900739 | -1.391976 | -1.061875 |
| H 5.162364 | -1.164121 | -0.02171 |
| H 5.471274 | -0.724475 | -1.722705 |

**Table S7** Cartesian coordinates for **2'**.

$E_{total}$ = -1291.964330 Hartree

| | | | |
|---|---|---|---|
| Si | -0.11716629 | -0.01426454 | -0.08190402 |
| C | 0.96477815 | -1.35028579 | -0.81490225 |
| C | 0.19497687 | 1.72540178 | -0.69131096 |
| C | 0.43132567 | -2.64067433 | -0.95435333 |
| H | -0.63955170 | -2.77643889 | -0.79670816 |
| C | 1.53585566 | 2.22477940 | -1.01198361 |
| C | 2.39534576 | -1.14317841 | -1.04747321 |
| C | -0.86845722 | 2.64545734 | -0.61594774 |
| H | -1.86172427 | 2.26494114 | -0.37225164 |
| C | 0.05937163 | -0.03787417 | 1.82060838 |
| C | -2.84761542 | -1.02639160 | 0.41875359 |
| H | -2.53371110 | -1.19433537 | 1.44677918 |
| C | -0.73787086 | 4.02213761 | -0.83518022 |
| H | -1.60307101 | 4.68312796 | -0.80304271 |
| C | -1.94100347 | -0.45788722 | -0.49167470 |
| C | 3.17823447 | -2.35807488 | -1.21459912 |
| H | 4.26393692 | -2.25606691 | -1.28353921 |
| C | 1.15287869 | -0.67611937 | 2.45196381 |
| H | 1.89235921 | -1.17850191 | 1.83163361 |
| C | 1.64190072 | 3.66250401 | -1.18323140 |
| H | 2.63454635 | 4.07048533 | -1.38833769 |
| H | -4.83579411 | -1.81687577 | 0.76857711 |
| C | 1.20042596 | -3.77807731 | -1.25366037 |
| H | 0.73924557 | -4.75933319 | -1.35516902 |
| C | -0.86714870 | 0.60977569 | 2.67961147 |
| H | -1.70366700 | 1.15619227 | 2.24695188 |
| C | 0.34921615 | -0.07419919 | 4.66927204 |
| H | 0.45847362 | -0.09186281 | 5.75341270 |
| C | 1.30399751 | -0.69064092 | 3.83957535 |
| C | -0.73663015 | 0.58000546 | 4.07012680 |
| H | -1.48054141 | 1.08100818 | 4.69167652 |
| H | 2.16362518 | -1.19560493 | 4.28126347 |
| C | -3.67239428 | -0.66833568 | -2.22143230 |
| H | -3.98171430 | -0.54044623 | -3.25943288 |
| C | -4.56196068 | -1.21402559 | -1.29044437 |
| H | -5.56789882 | -1.50547869 | -1.59681541 |
| C | 2.60969843 | -3.60746335 | -1.33336075 |
| H | 3.25595142 | -4.47595631 | -1.48635237 |
| C | -2.38398668 | -0.28507744 | -1.82004542 |
| H | -1.70729396 | 0.15998376 | -2.54702817 |
| C | 2.71964684 | 1.47220640 | -1.14973515 |
| H | 3.59551566 | 2.10577044 | -1.32299557 |
| C | 3.07488024 | 0.08929026 | -1.13130333 |
| H | 4.15317242 | -0.04480342 | -1.26918430 |
| C | 0.56757933 | 4.51972064 | -1.11302769 |
| H | 0.72385066 | 5.59046156 | -1.26606297 |
| C | -4.15060817 | -1.38906712 | 0.03596814 |

**Table S8** Cartesian coordinates for **4**.

$E_{total}$ = -937.461840 Hartree

| | | | |
|---|---|---|---|
| C | 2.481596 | -1.441241 | 0.248612 |
| H | 2.239814 | -2.507023 | 0.250506 |
| C | -1.464149 | -0.545765 | -0.076898 |
| C | 0.718876 | 1.895656 | -0.151554 |
| H | 1.137417 | 2.907996 | -0.196830 |
| C | -1.697538 | 0.899835 | -0.051485 |
| C | -0.718878 | 1.895656 | -0.151553 |
| H | -1.137420 | 2.907995 | -0.196832 |
| C | 1.464150 | -0.545765 | -0.076899 |
| C | 1.697536 | 0.899836 | -0.051480 |
| C | -2.481593 | -1.441241 | 0.248621 |
| H | -2.239809 | -2.507023 | 0.250521 |
| C | -3.101596 | 1.260813 | 0.056709 |
| H | -3.364001 | 2.315274 | -0.074878 |
| C | 3.801969 | -1.031202 | 0.528369 |
| H | 4.572799 | -1.753006 | 0.798578 |
| C | 3.101593 | 1.260816 | 0.056720 |
| H | 3.363997 | 2.315278 | -0.074861 |
| C | -4.096907 | 0.351886 | 0.360612 |
| H | -5.126702 | 0.705784 | 0.467894 |
| C | -3.801966 | -1.031202 | 0.528377 |
| H | -4.572795 | -1.753005 | 0.798592 |
| C | 4.096906 | 0.351888 | 0.360615 |
| H | 5.126700 | 0.705788 | 0.467900 |
| S | 0.000000 | -1.251118 | -0.841448 |

## 12. $^{1}H$, $^{13}C\{^{1}H\}$, $^{29}Si\{^{1}H\}$, $^{7}Li\{^{1}H\}$ NMR spectra for the new compounds

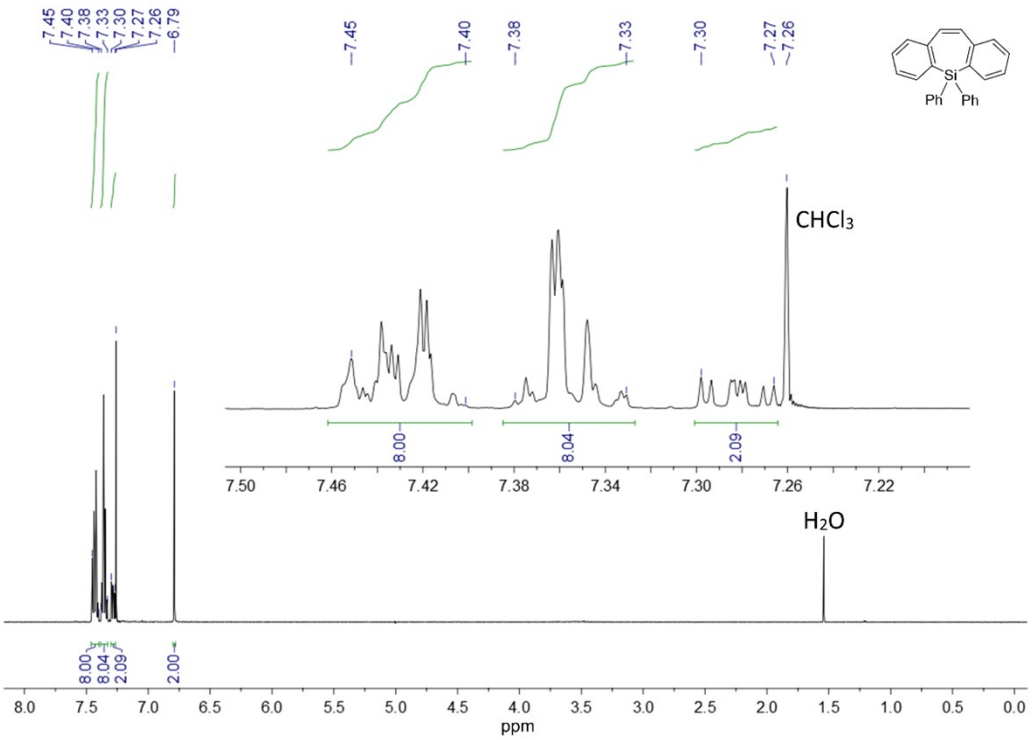


**Figure S6** $^{1}H$ NMR spectrum of **1** in $CDCl_3$.

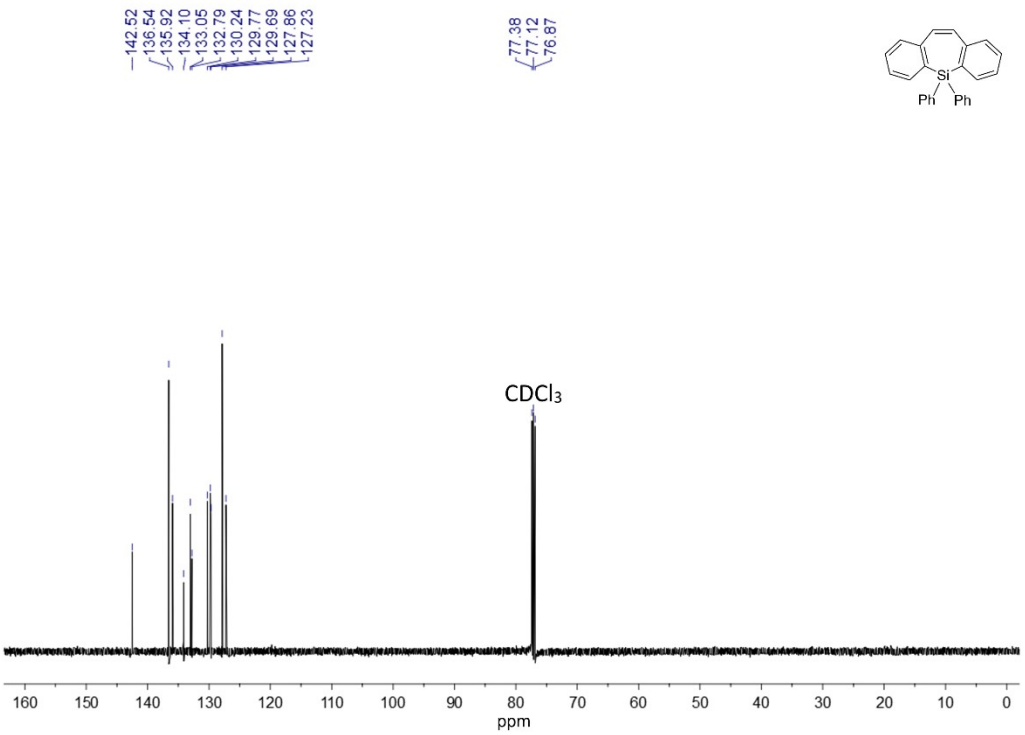


**Figure S7** $^{13}C\{^{1}H\}$ NMR spectrum of **1** in $CDCl_3$.

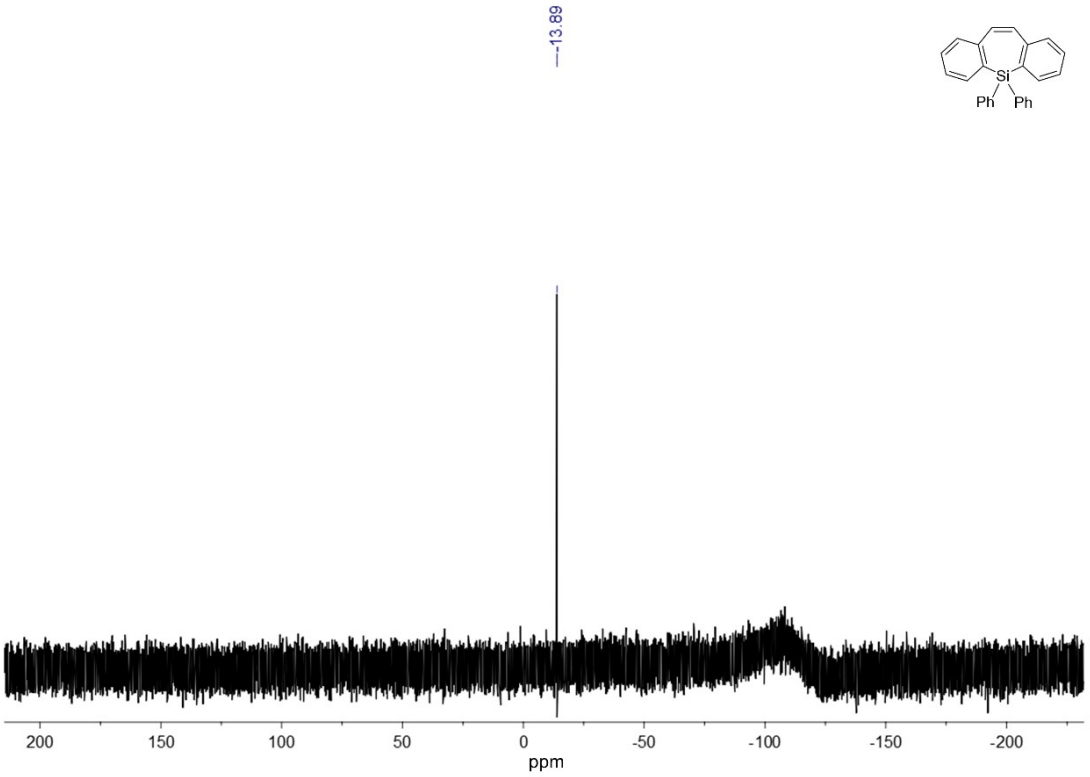


**Figure S8** $^{29}Si\{^{1}H\}$ NMR spectrum of **1** in $CDCl_3$.

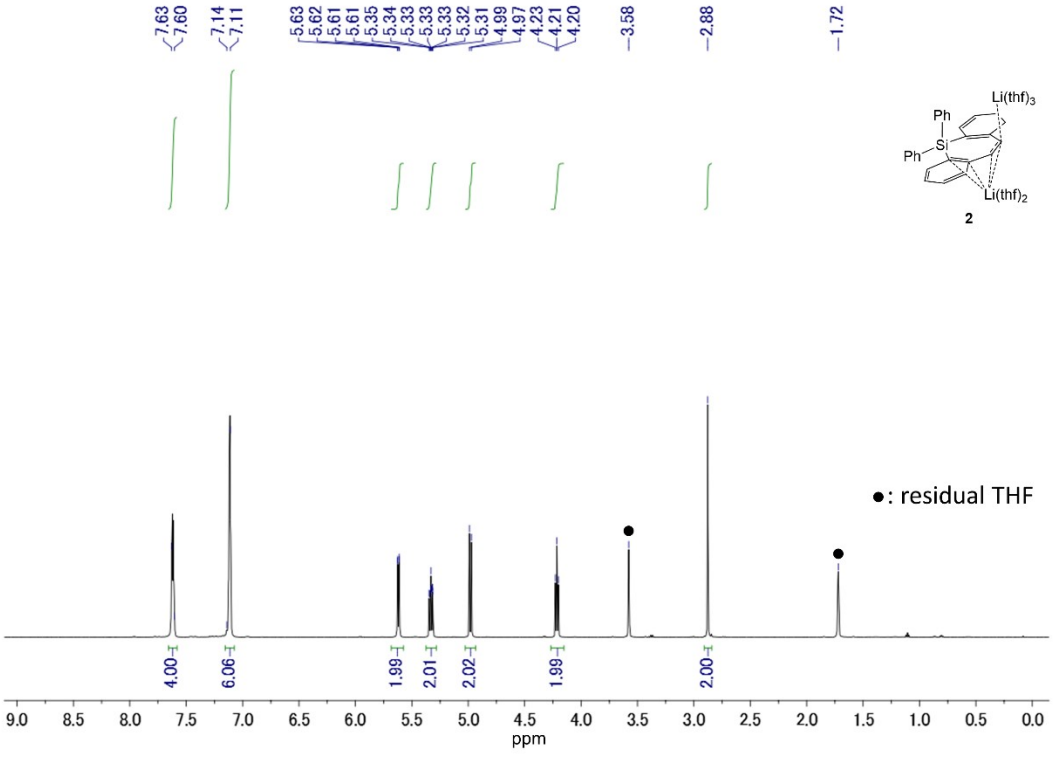


**Figure S9** $^{1}H$ NMR spectrum of **2** in THF-$d_8$.

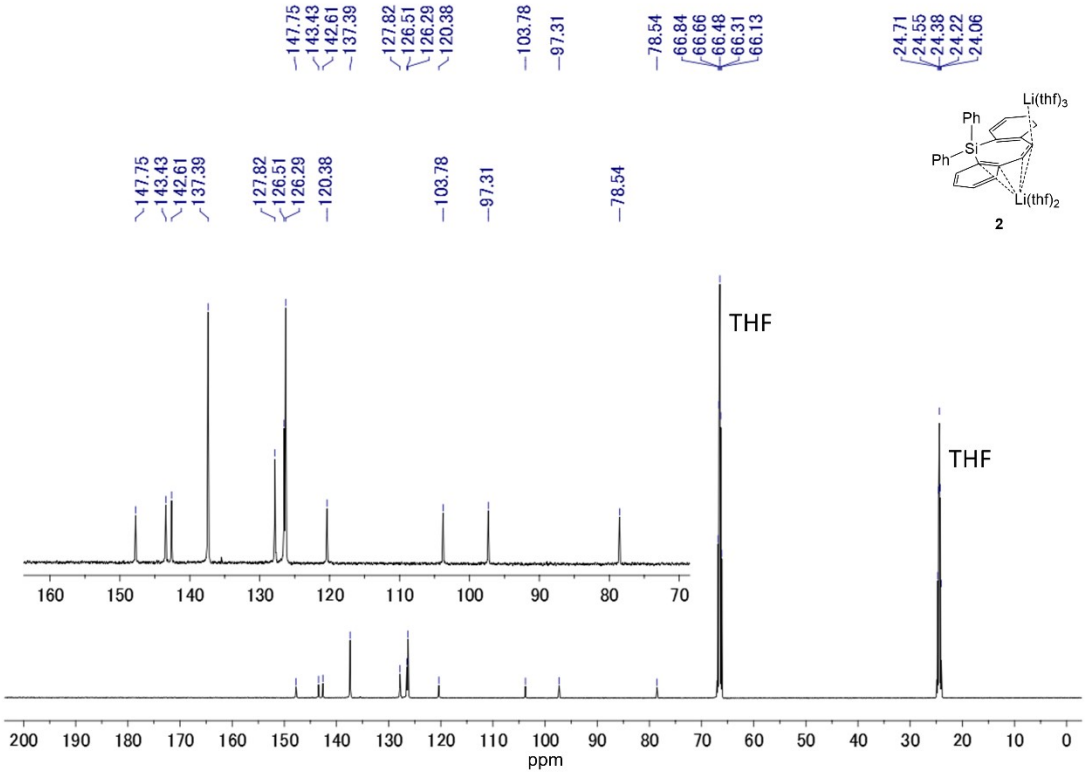


**Figure S10** $^{13}C\{^{1}H\}$ NMR spectrum of **2** in THF-$d_8$.

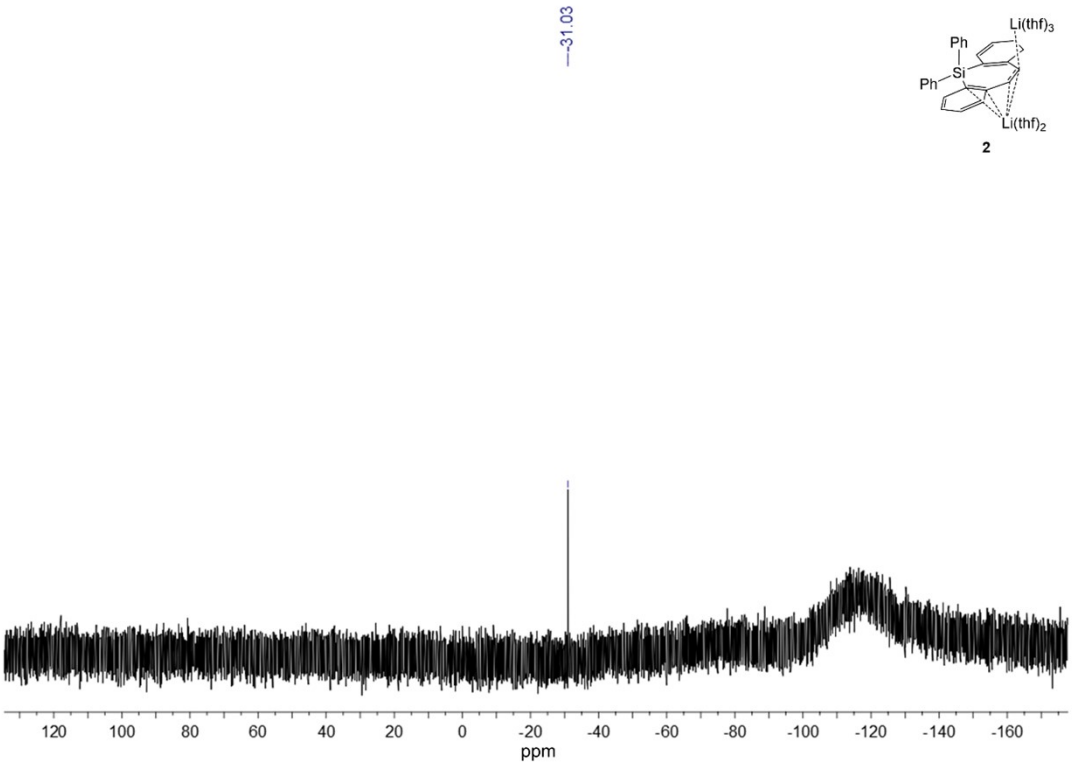


**Figure S11** $^{29}Si\{^{1}H\}$ NMR spectrum of **2** in THF-$d_8$.

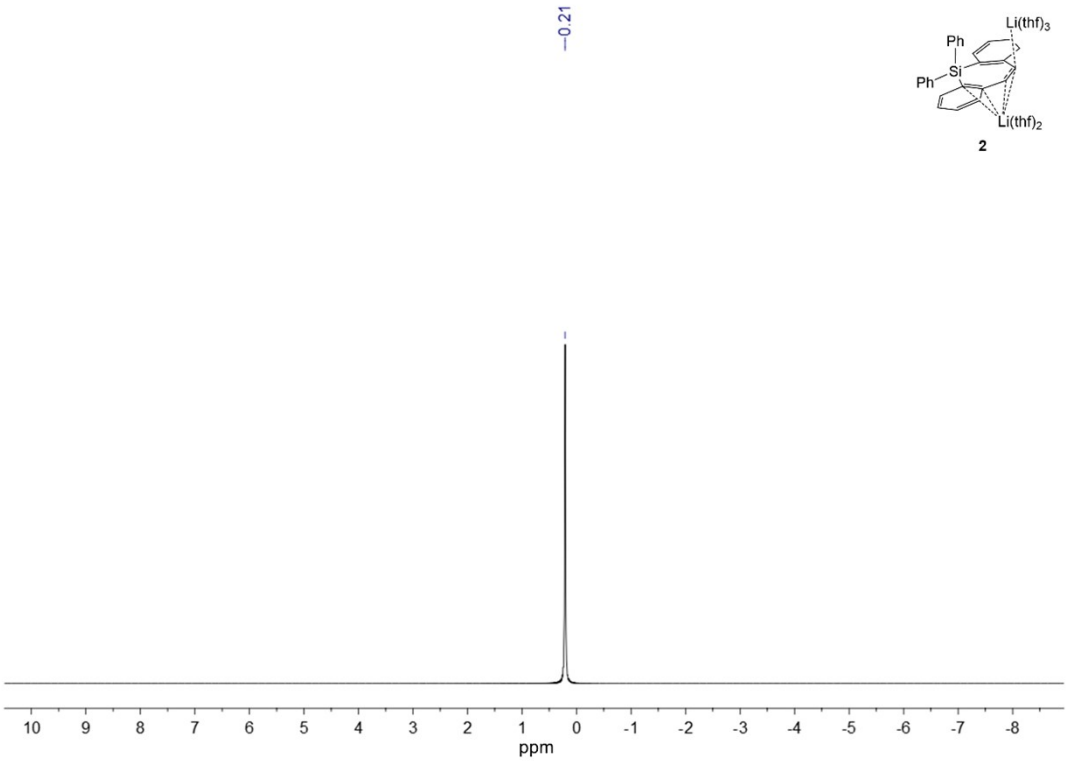


**Figure S12** $^{7}Li\{^{1}H\}$ NMR spectrum of **2** in THF-$d_8$.

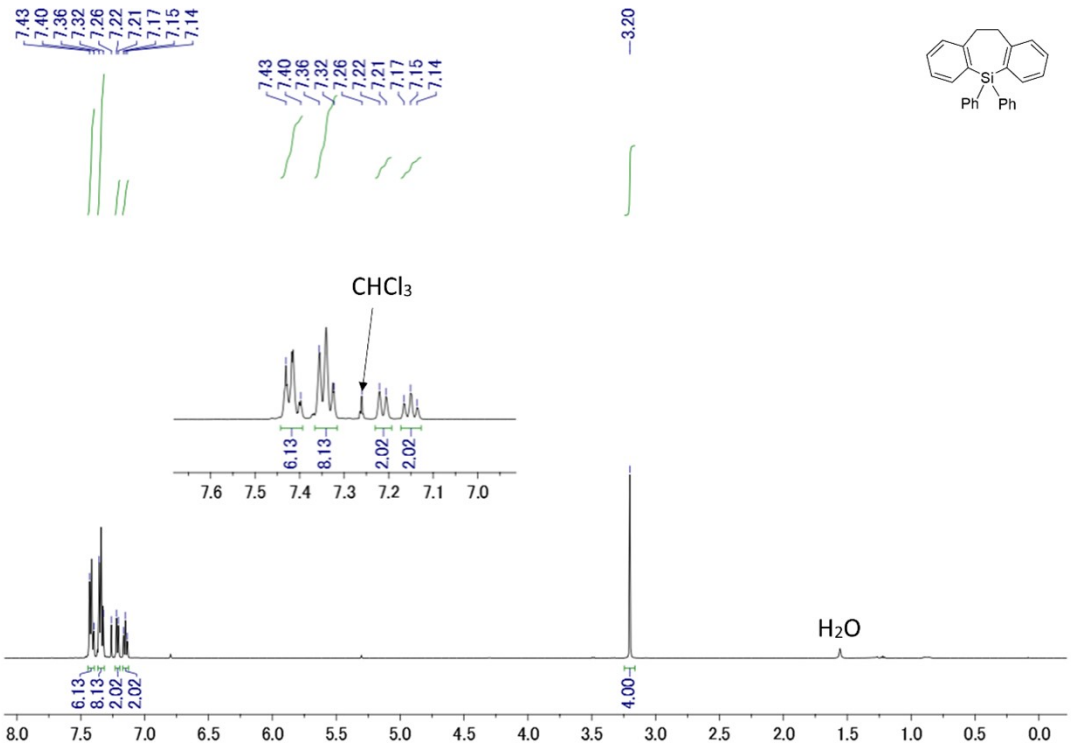


**Figure S13** $^{1}H$ NMR spectrum of **3** in $CDCl_3$.

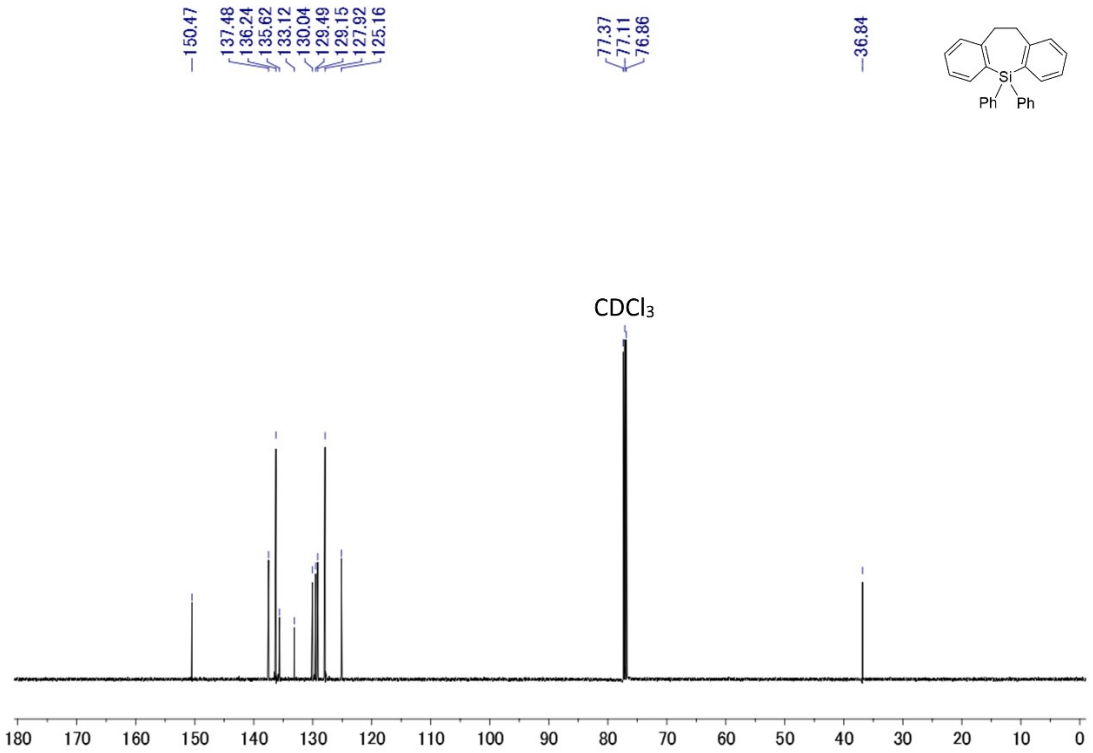


**Figure S14** $^{13}C\{^{1}H\}$ NMR spectrum of **3** in $CDCl_3$.

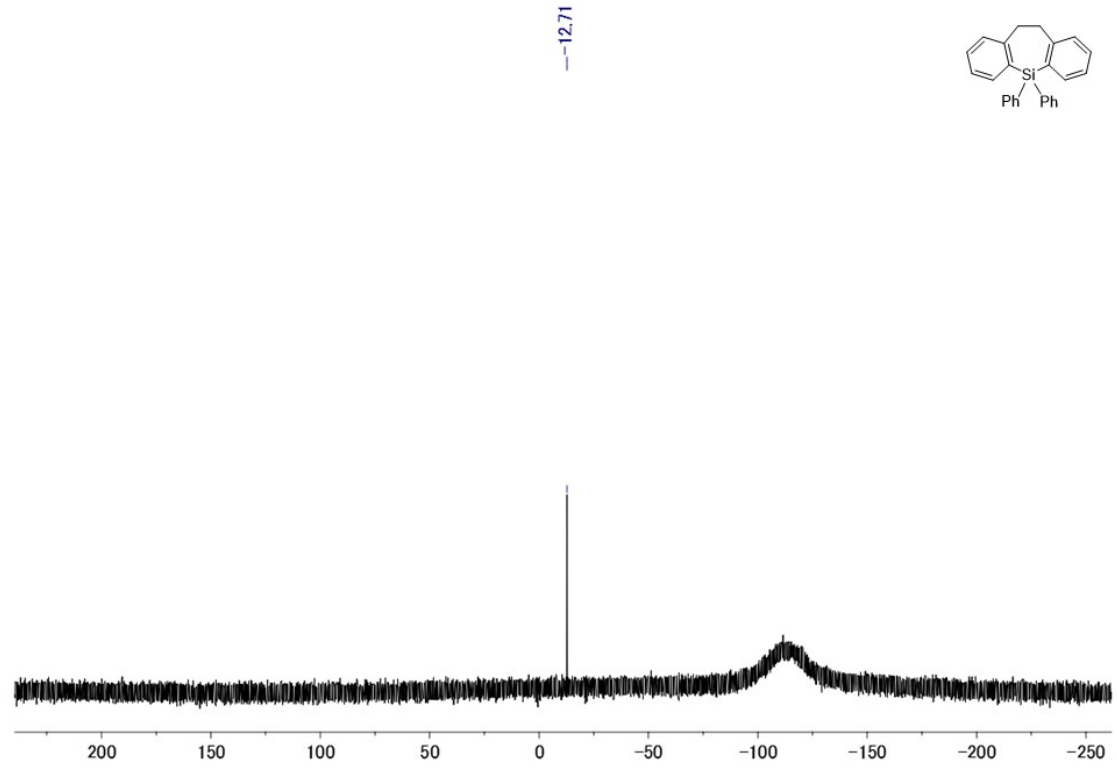


**Figure S15** $^{29}Si\{^{1}H\}$ NMR spectrum of **3** in $CDCl_3$.

## 13. References


1 L. G. Mercier, W. E. Piers and M. Parvez, *Angew. Chem., Int. Ed.*, 2009, **48**, 6108-6111.

2 R. A. Jacobson, *Private Communication to Rigaku Corp.; Rigaku Corp.; Tokyo Japan*, 1998.

3 *Crystal Structure 4.0: Single Crystal Structure Analysis Package; Rigaku Corp.; Tokyo, Japan* 2000-2010.

4 G. Sheldrick, *Acta Crystallogr. Sec. C*, 2015, **71**, 3-8.

5 A. Altomare, M. C. Burla, M. Camalli, G. L. Cascarano, C. Giacovazzo, A. Guagliardi, A. G. G. Moliterni, G. Polidori and R. Spagna, *J. Appl. Cryst.*, 1999, **32**, 115-119.

6 M. J. Frisch, G. W. Trucks, H. B. Schlegel, G. E. Scuseria, M. A. Robb, J. R. Cheeseman, G. Scalmani, V. Barone, G. A. Petersson, H. Nakatsuji, X. Li, M. Caricato, A. V. Marenich, J. Bloino, B. G. Janesko, R. Gomperts, B. Mennucci, H. P. Hratchian, J. V. Ortiz, A. F. Izmaylov, J. L. Sonnenberg, Williams, F. Ding, F. Lipparini, F. Egidi, J. Goings, B. Peng, A. Petrone, T. Henderson, D. Ranasinghe, V. G. Zakrzewski, J. Gao, N. Rega, G. Zheng, W. Liang, M. Hada, M. Ehara, K. Toyota, R. Fukuda, J. Hasegawa, M. Ishida, T. Nakajima, Y. Honda, O. Kitao, H. Nakai, T. Vreven, K. Throssell, J. A. Montgomery Jr., J. E. Peralta, F. Ogliaro, M. J. Bearpark, J. J. Heyd, E. N. Brothers, K. N. Kudin, V. N. Staroverov, T. A. Keith, R. Kobayashi, J. Normand, K. Raghavachari, A. P. Rendell, J. C. Burant, S. S. Iyengar, J. Tomasi, M. Cossi, J. M. Millam, M. Klene, C. Adamo, R. Cammi, J. W. Ochterski, R. L. Martin, K. Morokuma, O. Farkas, J. B. Foresman and D. J. Fox, *Gaussian 16 Rev. C.01*, Gaussian, Inc., Wallingford, CT, 2016.

7 M. J. Frisch, G. W. Trucks, H. B. Schlegel, G. E. Scuseria, M. A. Robb, J. R. Cheeseman, G. Scalmani, V. Barone, G. A. Petersson, H. Nakatsuji, X. Li, M. Caricato, A. Marenich, J. Bloino, B. G. Janesko, R. Gomperts, B. Mennucci, H. P. Hratchian, J. V. Ortiz, A. F. Izmaylov, J. L. Sonnenberg, D. Williams-Young, F. Ding, F. Lipparini, F. Egidi, J. Goings, B. Peng, A. Petrone, T. Henderson, D. Ranasinghe, V. G. Zakrzewski, J. Gao, N. Rega, G. Zheng, W. Liang, M. Hada, M. Ehara, K. Toyota, R. Fukuda, J. Hasegawa, M. Ishida, T. Nakajima, Y. Honda, O. Kitao, H. Nakai, T. Vreven, K. Throssell, J. J. A. Montgomery, J. E. Peralta, F. Ogliaro, M. Bearpark, J. J. Heyd, E. Brothers, K. N. Kudin, V. N. Staroverov, T. Keith, R. Kobayashi, J. Normand, K. Raghavachari, A. Rendell, J. C. Burant, S. S. Iyengar, J. Tomasi, M. Cossi, J. M. Millam, M. Klene, C. Adamo, R. Cammi, J. W. Ochterski, R. L. Martin, K. Morokuma, O. Farkas, J. B. Foresman and D. J. Fox, *Gaussian 09 Rev. E.01*, Gaussian, Inc., Wallingford CT, 2016.

8 (a) C. Lee, W. Yang and R. G. Parr, *Phys. Rev. B*, 1988, **37**, 785-789; (b) A. D. Becke, *J. Chem. Phys.*, 1993, **98**, 5648-5652.

9 Y. Zhu, Z. Zhou, Z. Wei and M. A. Petrukhina, *Organometallics*, 2020, **39**, 4688-4695.

10 R. Frim, A. Mannschreck and M. Rabinovitz, *Angew. Chem., Int. Ed. Eng.*, 1990, **29**, 919-921.

11 P. v. R. Schleyer, C. Maerker, A. Dransfeld, H. Jiao and N. J. R. v. E. Hommes, *J. Am. Chem. Soc.*, 1996, **118**, 6317-6318.